WildBridge: Conservation Software for Animal Localisation using Commercial Drones

K. Meier*, A. Richards, M. Watson, G. Maalouf, C. Johnson, D. Hine and T. Richardson
University of Bristol, Queens Road, Bristol, BS8 1QU, United Kingdom

http://www.imavs.org/

ABSTRACT

This paper assesses the usability and accuracy of a commercially off-the-shelf (COTS) platform for precise terrestrial animal localization. To achieve localization, this paper uses a single-shot coordinate transform method. The platform selected in this work is the DJI Mavic 3E quadcopter, since it is a popular and widely adopted platform, in particular among the wildlife conservation community. To enable the use of the DJI Mavic 3E, a software interface was developed to access telemetry and camera feed in realtime. The method was tested during two field campaigns in Kenya and Wales. These field campaigns permitted the discovery of localization error sources and their possible mitigation, in particular through adequate mission planning. The preliminary maximum localization error was computed to be 19.2m laterally and 14.4m longitudinally for an animal positioned 385m from the UAV flying at 120m above ground.

1 INTRODUCTION

1.1 Overview

Recent developments in Computer Vision (CV) and Unoccupied Aircraft System (UAS) have offered the potential for providing a step-change in animal conservation through automated monitoring of wildlife from the air – yet despite many successful deployments, the true potential of the concept has yet to be realised [1].

This paper will provide a stepping stone on the front of animal detection and localization. More specifically, this paper has three technical aims: (i) interface with a commercial platform (DJI Mavic 3E) from a local computer to provide real-time detection and localisation of large mammals, (ii) evaluate the localisation accuracy of the observed animals and identify the error sources, (iii) provide recommendation for the deployment of this system in the field.

WildBridge is the name of the system that brings these three goals together to create an integrated system for real-time localization of animals using Commercial Off The Shelf (COTS) drones. The WildBridge user interface can be seen in Figure 1.

*Email address: kilian.meier@bristol.ac.uk

1.2 Background

It is estimated that one-fifth of the world's vertebrate species are currently threatened with extinction [2], consequently, the need for more effective means of surveying wildlife populations has never been so important. Wildlife is traditionally monitored primarily either by foot, car, ship, crewed aircraft, or more recently using camera traps. However, these methods are often expensive, time-consuming, and logistically difficult in remote areas, making the monitoring and assessment of biodiversity one of the biggest challenges in modern conservation. Effective wildlife monitoring and adaptive management critically depend on regular surveys of wildlife abundance [3]. Aerial monitoring has the potential to provide frequent and systematic surveys.

There are three primary means by which aerial imagery can be gathered for conservation purposes: crewed aircraft, satellites and UAS/drones.

For large African landscapes, manual aerial surveys with light aircraft are still considered the best method of counting large mammals [4], [5]. However, high costs and logistical constraints mean that light aircraft surveys either do not take place at all, or if they do, the time between successive surveys is so long that catastrophic declines in populations can occur [6].

Commercially available high-resolution imagery from satellite sensors including Quickbird, GeoEye-1 and World View-3 and 4 have been successful in estimating abundances of large mammals in savannahs [7], [8]. However, obstruction of view caused by vegetation in complex wooded savannah environments limits their application and the lack of very high-resolution imagery prevents individual animal identification [8].

Unlike satellite imagery, aerial surveys using UAS/drones can provide an oblique view in complex habitats providing superior images for wildlife detection and the identification of individual animals [9]. UAS can be deployed quickly, fly autonomously, and collect high-resolution aerial imagery, making them a key candidate for detecting and counting wildlife [10]. In the last 20 years, UAS technologies have advanced substantially and the subsequent decreases in cost have made them more readily accessible in the field of conservation. Consequently, several key areas have been highlighted within conservation where UAS might provide great benefit, e.g. the real-time mapping of land cover, monitoring of illegal deforestation, detection of poaching activities, and wildlife surveying [11], [12], [13]. More specifically,

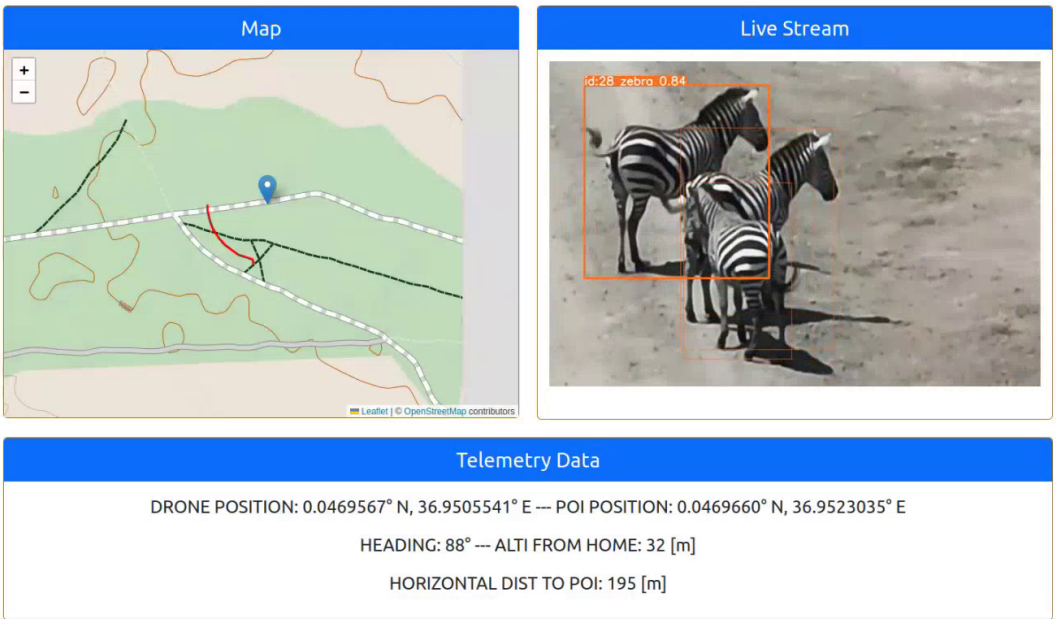

Figure 1: WildBridge web-based graphical user interface. The left tile shows the localization results on a map: the red line is the drone trajectory (the drone is at the top left of the curve) and the blue pin represents the estimated location of the animal. The right tile shows the live camera feed and highlights the localized animal. The bottom tile displays selected telemetry. This snapshot was taken during a flight in Ol Pejeta Conservancy, Kenya.

http://www.imavs.org/

ecologists have successfully used UAS to survey a variety of taxa, including several bird species (Canada geese, snow geese, and white ibis) [14]; great ape nests [15]; salmon [16]; and manatees [16]. A variety of sensors have also been utilized with good effect including thermal [17] and audio recorders [18]. Recent developments in deep learning image recognition can now automatically count animals from aerial images in open and homogenous landscapes [19], [20].

1.3 Problem Formulation

The task at hand is to automatically and in real-time determine the geographic location of the POI, given the knowledge of the drone's geographic location, the camera orientation, the camera parameters and the location of a POI in the image. To access the data needed for the localisation, a system must be built to have real-time access to a drone's telemetry and camera feed. In order to make this system easy to use, robust and accessible, three main design choices have been made. First, WildBridge has been developed for the DJI Mavic 3E quadcopter (see Section 2.2), which is a widely used platform in conservation due to its price, ease of use and robustness [21], [22]. Second, the software stack has been mainly written in Python, which is a popular language due to its ease of use and allows WildBrige to be easily upgraded and customized according to the user's need.

The rest of the paper will be organised as follows. Section 1.4 explores the state of the art, further assessing the need for a tool like WildBridge, as well as listing the different tools and methods already in use by conservationists. Section 2 provides an overview of the different components of WildBridge and how they interact. This section also presents how WildBridge can be adapted to different platforms and tailored for different needs. Section 3 describes how the localisation is performed. Section 4 presents preliminary results based on data collected by WildBridge and discusses the nature and magnitude of measurement errors. Finally, Section 5 concludes and presents further development directions of WildBridge.

1.4 State of the Art

Several research groups have tried to address the question of localizing animals using UAS. In particular, several conservation groups have used mapping techniques or orthographic photos to count, locate and measure animals in optical images: such as various crocodylians [21], European brown hare (*Lepus europaeus*) [23] or Black-Necked Swan (*Cygnus melancoryphus*) [24]; and thermal images: northern bobwhite quail (*Colinus virginianus*) [17]. The benefit of using nadir imagery is the simplification of the problem's geometry and ensures a well-known Ground Sample Distance (GSD), thus enabling size measurements [21]. It also leverages well-established mapping tools such as Pix4D (Prilly, Switzerland, pix4d.com). However, generating a map is computationally intensive and does not allow real-time localization and mapping. Moreover, the requirement for nadir images and a specific overlap constrain flight operations and

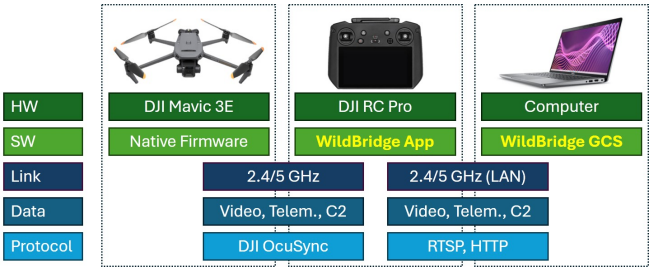

Figure 2: WildBridge system block diagram. store.dji.com, etrix.com.sg

does not give the user the flexibility to react to unexpected changes during the survey.

A different problem which has, however, a related solution is the problem of UAS localization in GNSS-denied environments. There are several approaches to solve this problem, but one of them is triangulating the UAS position from known reference points [25] and [26]. The geometry of the problem is the same, but the unknown is the UAS position instead of the animal position (reference point).

It is also worth mentioning that using image-based techniques is not the only viable approach to animal localization. Radio-based approaches have also proven to be effective [27] and have led to companies offering it as a service, such as Wildlife Drones (Acton, Australia, wildlifedrones.net). Radio location has the benefit of not relying on any resource-intensive image processing pipeline, of being able to identify specific individuals, and of permitting reliable localization in occluded and dense environments. It comes however at the cost of having to tag the animals to be tracked, which might be difficult or even impossible. DJI has also released a laser-based approach, enabling the localisation of POIs seen by the drone (DJI PinPoints). To achieve this, a laser range finder is used to measure the distance between the drone and the POI. This distance is then used to localise the POI based on the drone's position and orientation.

Finally, authors in [28] investigated the use of UAS to locate invasive trees (*Miconia calvescens*) using a similar approach to the one presented in this work. However, in [28], the localization is performed in post-processing.

Note that most papers cited in the section use DJI drones, which suggests their adequacy for wildlife conservation applications.

2 EXPERIMENTAL SETUP

2.1 Overview

Figure 2 shows an overview of WildBridge and the following sections describe each component of the system.

2.2 Drone platform

The UAV selected for this work is the DJI Mavic 3 Enterprise (Figure 2). A summary of its specifications can be found in Table 1. The platform was selected due to its wide use and its proven record in remote and harsh environments. In addition, it features high-quality cameras with a zoom capacity of up to x56, which is ideal for animal surveys while avoiding any disturbances on the animals. While this platform has been selected for its high performance, WildBridge should be compatible with all DJI products supporting Mobile SDK V5[1], i.e. Mavic 3, Mini 3 and Matrice 300 series (see Section 2.3 for more details about the SDK). However, WildBridge has not been tested on any of those platforms yet.

Aircraft	Weight	915 g
	Diagonal	380.1 mm
	Max hover time	38 min
Wide cam.	Sensor	4/3 CMOS, 20 MP
	Lens FOV	84°
	Lens format equi.	24mm
	Lens aperture	f/2.8-f/11
	Video resolution	FHD or 4K at 30fps
Tele cam.	Sensor	1/2-inch CMOS, 12 MP
	Lens FOV	15°
	Lens format equi.	162mm
	Lens aperture	f/4.4
	Video resolution	FHD or 4K at 30fps
	Digital Zoom	8x (56x hybrid zoom)

Table 1: DJI Mavic 3E specifications. Summarised from https://enterprise.dji.com/mavic-3-enterprise/specs.

2.3 Remote Controller (RC)

The RC selected for this work is the DJI RC Pro (Figure 2. This is the default controller delivered with the DJI Mavic 3E. Importantly, the RC runs on Android and supports DJI's Mobile SDK V5 (MSDK). This Software Development Kit (SDK) provides an interface to the drone and thus enables the WildBridge app to access the drone's telemetry and video streams, and send control commands back to the drone. The RC communicates with the drone over a 2.4 GHz and a 5 GHz radio link and with the GCS laptop via a Local Area Network (LAN).

2.4 WildBridge app

The WildBridge app is the actual "bridge" of the project. It enables any device on the LAN to receive telemetry data and to send control commands from and to the drone. This is achieved by implementing an HTTP server answering to telemetry and control command requests. The WildBridge app also runs an RTSP server broadcasting the drone's camera feed. The app is written in Java and Kotlin and has been adapted from the MSDK's example application[2]. The telemetry fields accessed in this work over the MSDK are KeyAircraftLocation3D, KeyAircraftAttitude, KeyGim-

[1] https://developer.dji.com/mobile-sdk/
[2] Mobile-SDK-Android-V5

http://www.imavs.org/

http://www.imavs.org/

balAttitude and KeyCameraZoomRatios[3]. Note, that this implies that the drone cannot be flown using the native Pilot 2 app and the WildBridge app must be used instead for piloting.

2.5 Laptop

In this work, a Dell Inc.Latitude 5440 operating on Ubuntu 22.04.4 LTS was used and was able to perform around 4 to 5 localizations per second. However, most modern computers can be used as long as they can access the LAN and can run Python scripts. Given that the computer is running an object detection algorithm it is recommended the computer has reasonable image processing capabilities. This machine also hosts the web-based user interface, displaying the localization results (Figure 1).

3 METHODOLOGY

3.1 Notations and reference frames

A vector $\mathbf{r}$ in a frame f is noted as $\mathbf{r^f}$. A rotation matrix $\mathbf{C}$ transforming a vector from frame a to b is noted as $\mathbf{C_a^b}$, i.e. $\mathbf{r^b} = \mathbf{C_a^b r^a}$.

There are three reference frames to consider: the image frame (i), the camera frame (c) and the world frame (w). The image frame is a two-dimensional frame, spanning the camera sensor plane. Its origin is in the top left corner of the image. The camera frame has its origin at the focal point of the camera and is oriented such that its y- and z-axis are parallel to the x- and y-axis of the image frame, respectively. The camera frame's x-axis is perpendicular to the sensor plane and crosses it in its centre (see Figure 3). The distance between the origin of the camera frame and sensor plane and the focal length. Finally, the world frame's x-, y- and z-axis are aligned with the North, East and Down cardinal directions.

3.2 Localisation

The localisation problem can formulated as finding the relationship between a POI detected in the image and a POI in the world. Let's call the former the virtual POI (vPOI) and the latter the world POI (wPOI).

Assuming a vPOI has been found in the image frame, locating it in the world can be achieved by tracing a ray originating from the camera focal point (origin of the camera frame) and passing through the vPOI. The intersection between this ray and the ground is the location of the wPOI (see Figure 3). Hence, this section needs to derive a parameterization of this ray in the world frame. Thus, let's assume a known vPOI in the image frame such that:

$$\mathbf{r^i_{vPOI}} = \begin{bmatrix} x^i_{vPOI} \\ y^i_{vPOI} \end{bmatrix} \tag{1}$$

where x^i_{vPOI} and y^i_{vPOI} are expressed in meters. However, the position of the detected POI in the image is measured in pixels. The conversion can be achieved by knowing the physical size of a pixel in the camera sensor. For the zoom lens of the DJI Mavic 3E used in this work, the pixels have a length $s = 1.6\ [\mu m]$[4]. Thus:

$$\mathbf{r^i_{vPOI}} = \begin{bmatrix} x^i_{vPOI} \\ y^i_{vPOI} \end{bmatrix} = s \cdot \mathbf{r^i_{vPOI,pix}} \tag{2}$$

where $\mathbf{r^i_{vPOI,pix}}$ is the position of the vPOI in the image frame expressed in pixels.

Then the position of the vPOI in the camera frame can be expressed as:

$$\mathbf{r^c_{vPOI}} = \begin{bmatrix} f \\ x^i_{vPOI} - W/2 \\ y^i_{vPOI} - H/2 \end{bmatrix} \tag{3}$$

where W and H are the total image width and height respectively and f the camera's focal length. Hence a parametric line $\mathbf{d}$ originating from the camera origin and passing through the vPOI can be written as:

$$\mathbf{d}(\lambda)^\mathbf{c} = \lambda \mathbf{r^c_{vPOI}} \tag{4}$$

Where λ is the parameter. Now let's express this line in the world frame:

$$\mathbf{d}(\lambda)^\mathbf{w} = \lambda \mathbf{C^w_c r^c_{vPOI}} + \mathbf{r^w_c} \tag{5}$$

where $\mathbf{r^w_c} = [n_c\ e_c\ d_c]^T$ is the known translation of the camera frame with respect to the world frame and $\mathbf{C^w_c}$ is the rotation matrix encoding the relative orientation of the world

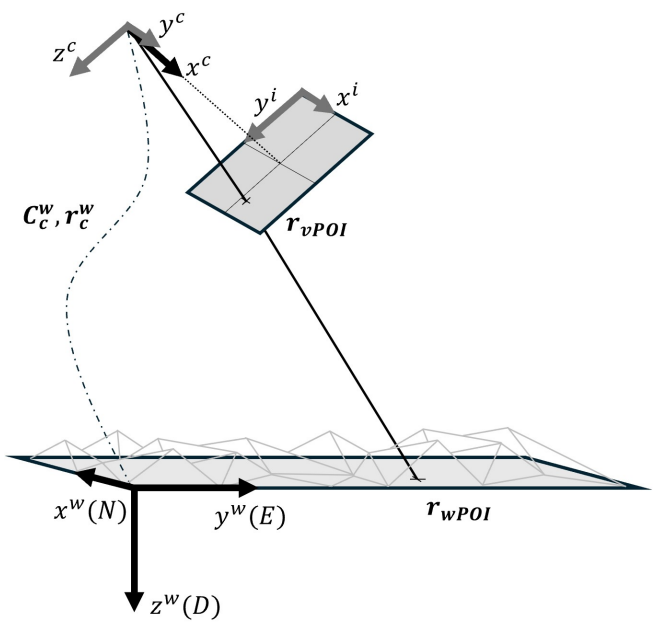

Figure 3: Reference Frames.

[3]DJI MSDK Documentation

[4]Calculated from the surface each pixel covers based on the DJI Mavic 3E specifications.

http://www.imavs.org/

frame with respect to the camera frame. This rotation can be expressed as an intrinsic "zy" rotation[5]:

$$\mathbf{C_c^w} = \mathbf{C_z}(\psi)\mathbf{C_y}(\theta) = \begin{bmatrix} c_\psi c_\theta & -s_\psi & c_\psi s_\theta \\ s_\psi c_\theta & c_\psi & s_\psi s_\theta \\ -s_\theta & 0 & c_\theta \end{bmatrix} \tag{6}$$

where ψ is the camera heading, θ is the camera pitch and s and c represent the sine and cosine functions of the subscripted angle. Finally, the intersection between $\mathbf{d}(\lambda)^\mathbf{w}$ and the ground can be expressed as:

$$\mathbf{d}(\lambda)^\mathbf{w} = \mathbf{r_{wPOI}^w} = \begin{bmatrix} n_{wPOI} \\ e_{wPOI} \\ d_{wPOI} \end{bmatrix} \tag{7}$$

where n_{wPOI} and e_{wPOI} are the northing and easting of the wPOI, which are unknown, and d_{wPOI} the elevation of the wPOI. The elevation could be known using a digital elevation model of the area of interest and then finding the intersection of the traced ray and the elevation map. However, this is outside of the scope of this paper. Hence, it is assumed the terrain is flat and since the POIs are animals evolving on the ground $d_{wPOI} = 0$. This is a strong assumption and a major source of error and will be address in future work. Thus, assuming $d_{wPOI} = 0$, (7) is a system of three equations with three unknowns: λ, n_{wPOI} and e_{wPOI}. Solving for λ leads to:

$$\lambda = \frac{d_c}{c_\theta(y^i_{vPOI} - H/2) - s_\theta f} \tag{8}$$

Explicit solutions for n_{wPOI} and e_{wPOI} can be expressed using (5) and (7). This system is solvable as long as:

$$c_\theta(y^i_{vPOI} - H/2) - s_\theta f \neq 0 \tag{9}$$

i.e. as long as the ray is not horizontal. The system has 11 parameters: x^i_{vPOI}, y^i_{vPOI}, s, f, W, H, n_c, e_c, d_c, ψ and θ.

4 RESULTS AND DISCUSSION

4.1 Ol Pejeta (Kenya) test campaign - Proof of concept

WildBridge has been tested during two different test campaigns with different aims and objectives. The first campaign took place in the Ol Pejeta Conservancy in Kenya and aimed at testing WildBridge in an environment representative of what conservationists may experience during their fieldwork. It was also an opportunity to present this work to the rangers and researchers of Ol Pejeta and discuss potential further developments of WildBridge.

Four flights were performed at various locations in the park, mainly observing zebras. The flights were conducted within visual line of sight (VLOS) since the WildBridge app does not yet implement some critical safety features to enable Beyond Visual Line of Sight (BVLOS) flights. To ensure the regulatory compliance of those flights, a Specific Operational Risk Assessment (SORA) [29] was submitted to both the Kenya Civil Aviation Authority (KCAA) [6] and the Kenyan military, since Ol Pejeta is a military controller airspace.

A snapshot of the WildBridge interface during one of the flights can be seen in Figure 1. Some flights were also live-streamed using Starlink to Ol Pejeta's control room, thus giving live information about animals in the park to the rangers. Note, however, that the accuracy of the localization was not assessed here due to the challenges related to the acquisition of a ground truth.

The main takeaways from this campaign are:

- The system was successfully used in a remote environment with real animal observations.
- The system awoke the interest of Ol Pejeta's rangers and has the potential to be integrated with Earthrange[7], Ol Pejeta's current monitoring interface.
- The WildBridge app, while being useable, should improve its user interface to enable safer piloting of the drone.
- The regulatory approval was more complex and time-consuming than expected due to the involvement of multiple stakeholders. Future missions should allocate sufficient contingency time for potential delays.

4.2 Llanbedr (Wales) test campaign - Characterisation

The second test campaign took place at Llanbedr Airfield in Wales and aimed at evaluating and characterising the localisation error of WildBrige. To achieve this, several flights were performed looking at a stationary POI on the ground, placed at a known location. The flights were flown manually and such that the POI was kept in the frame. All flights were achieved by controlling only two of the five control inputs available on the DJI RC Pro and they can be grouped into four categories: straight horizontal flight away or towards the POI (vertical left stick and gimbal pitch), straight ascent or descent (vertical right stick and gimbal pitch), diagonal flight away or towards the POI (vertical right and left stick), and orbit around the POI (horizontal left and right stick). In addition to those four flight types, flights were also performed only using one of the five available control inputs, but they are limited in range since they cannot control the POI to stay in the frame. These flights will be used in two different ways, first to understand and compensate for the limitations of the localisation method, second to make a first evaluation of the accuracy this system can achieve. Two sample flights can be seen in Figure 8 and 9.

[5]The camera is controlled such that its roll is always zero, hence the absence of an "x" rotation.

[6]https://kcaa.or.ke/

[7]EarthRanger website

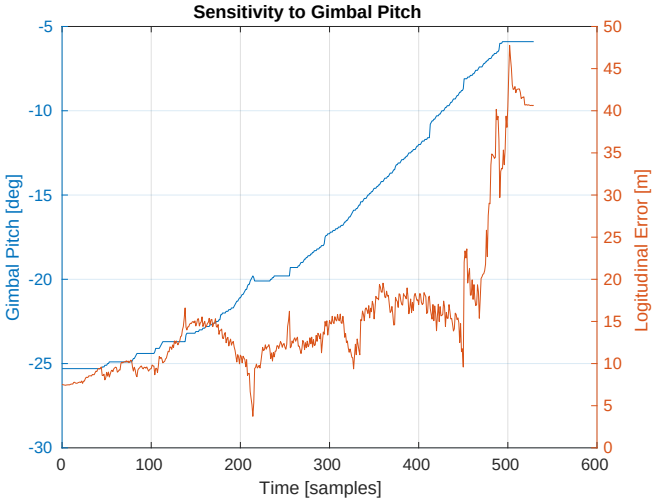

Figure 4: Correlation between pitch angle and longitudinal error during a vertically descending flight.

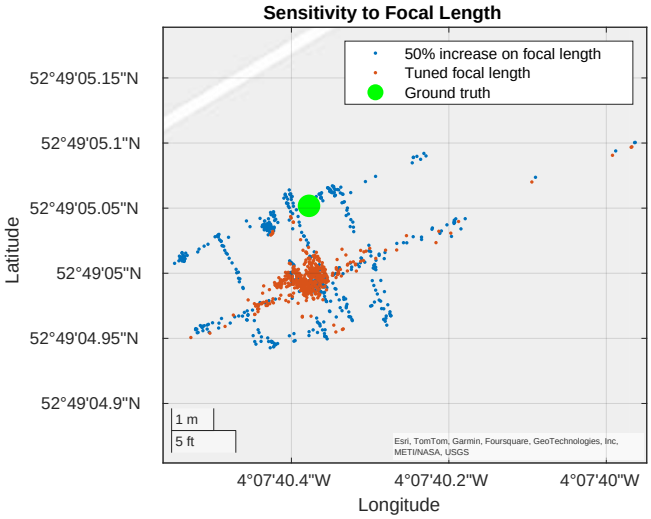

Figure 5: Impact of focal length tuning on localisation estimate during a stationary flight featuring yawing and gimbal pitching movements.

4.3 *Error definition*

The performance metric chosen in this work is lateral and longitudinal error with respect to the azimuth between the drone and the ground truth. In other words, the longitudinal error is the projection of the error vector on the horizontal axis connecting the ground truth point and the drone's position on the ground. The lateral error is the projection on an axis perpendicular to the longitudinal axis.

4.4 *Sensitivity to gimbal pitch error*

As described in Section 3.2, (7) is only solvable when the ray is not horizontal. But it is also worth noting, that for rays close to horizontal, the denominator in (8) is close to zero, making λ very sensitive to small errors in gimbal angle or vPOI detection and thus leading to large errors in the position estimation of the wPOI. This can be illustrated by looking at a vertically descending flight as shown in Figure 4. During the descent from approximately 120m to 20m above ground, the gimbal is operated such that the POI always stays in the field of view. As expected, the longitudinal error increases with decreasing gimbal angle.

4.5 *Sensitivity to focal length*

Unless the vPOI is in the centre of the image, the localisation estimate is dependent on the focal length (and more generally on the camera model used). DJI's MSDK enables access to several measurements of focal length, but after inspection of the data, it is unclear how any of the available values relate to the true focal length of the camera. Hence, in this work, the focal length used is the telemetry field named *KeyCameraZoomRatios*[8] scaled by a manually tuned parameter such that the localisation error is minimized. To illustrate the impact of the focal length tuning, Figure 5 shows two sets of localisation estimates, first with the manually tuned focal length, then with a 50% increase of the focal length. The flight in this example is a stationary flight during which the camera has been moved such that the POI draws a cross and a square in the image frame. The structure present in the estimation of the artificially increased focal length replicates the path drawn by the POI on the image frame. This results from the algorithm being unable to compensate for the displacement of the vPOI in the image frame.

[8]DJI MSDK Documentation KeyCameraZoomRatios

4.6 *Sensitivity to image and telemetry sychronisation*

For a correct localisation, all the data used by the algorithm must be time synchronised. Given that image and telemetry are broadcasted over different channels, they are the most at risk of suffering from synchronisation issues. To verify this, the vertical position in the image frame of the vPOI has been overlayed on the gimbal pitch angle during a stationary flight (Figure 6). It is clear in this example that the gimbal pitch signal is leading the object position in the image signal. Measurement of this delay resulted in approximately 4 samples ($\approx$ 1s) and all the data in this work has been shifted by this amount. The reason for this delay is that images are only timestamped once received by the GCS, but their transfer (including compression and decompression) takes time and this duration can vary depending on the network setup, the traffic on the network and the size or even content of the images. It is unclear whether it is possible to properly timestamp images before sending them, but this would be the best way to measure and compensate for this delay.

4.7 *Gimbal heading measurement*

DJI's MSDK allows the user to access a parameter named *KeyGimbalAttitude*, which according to the SDK's documen-

http://www.imavs.org/

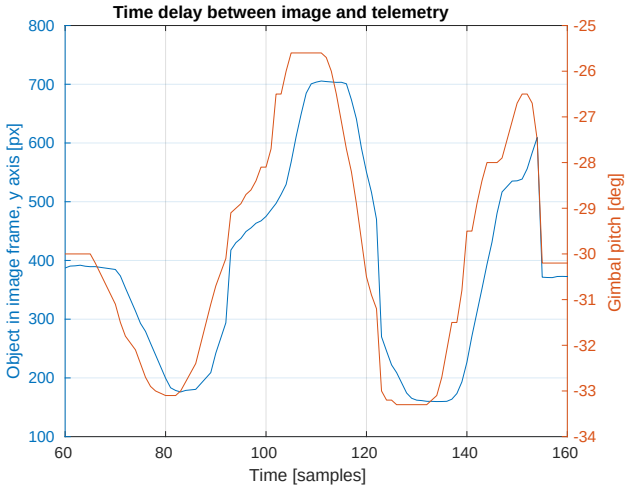

Figure 6: Vertical position in the image frame of the vPOI overlayed on gimbal pitch angle during a stationary flight, before time delay compensation.

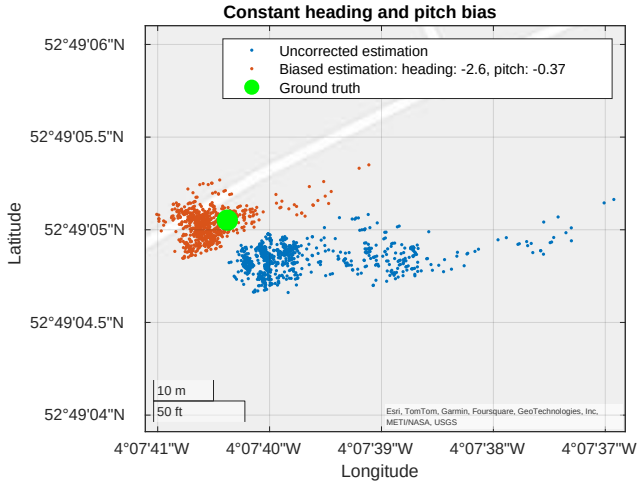

Figure 7: Impact of constant heading and pitch bias on localisation estimate during a 30m altitude flight toward the POI. Biased estimates feature a constant heading and pitch bias and were computed to minimize lateral and longitudinal error respectively.

tation[9] describes the heading of the camera in a NED world frame. However, after inspection of the data, this was not true in certain conditions. Thus, in this work, the drone heading was used (body heading). While this is not the true value, it is a fair approximation since the gimbal heading is controlled to be aligned with the forward direction of the drone and uses this degree of freedom only to smooth out yawing movements. In other words, gimbal heading and drone heading are equal when the drone is not yawing, but their difference may be high during yawing movements.

4.8 *Heading and pitch biases*

Figure 7 shows the localisation estimate (in blue) for a straight flight towards the POI (in green). Computing the heading bias to minimize the lateral error and the pitch bias to minimize the longitudinal error leads to the biased estimates (in red). The fact that biased estimate collapses to an ellipsoid around the ground truth, suggests that there is indeed a constant error in the heading and pitch measurements. Comparing this bias on different flights unfortunately leads to the conclusion that these biases are not constant across different missions. A possible explanation for this observation is that relative encoders are used in the drone's gimbal, which are well suited for filming since they can be used to stabilise the camera. However, relative encoders are sensitive to their initialization routine and may drift over time if steps are miscounted. This could be mitigated by including a calibration routine in the drone's flight. For example, by localising the pilot holding the remote controller which features a GNSS receiver and thus can be used as a ground truth.

[9]DJI MSDK Documentation KeyGimbalAttitude

4.9 *Mission planning recommendation*

While the contributions of the error sources listed above could be mitigated by a better understanding of the system or by an improved processing pipeline, they can also be mitigated during mission planning. Hereafter, are three recommendations that can improve the estimation accuracy.

- Ensure that the gimbal pitch is as close to vertical as possible, either by flying higher or closer to the POI (see Section 4.4). This is limited by other requirements, such as image quality, safety distance to the POI or compliance with regulations (altitude ceiling).
- Keep the POI as close to the image centre as possible, thus mitigating the impact of lens distortion and error in the focal length (see Section 4.5). However, this might be hard to achieve during manual flight or even impossible when looking at multiple POIs.
- Make slow movements and maximise stationary observations. This reduces the impact of bad telemetry synchronisation (see Section 4.6).

4.10 *Performance evaluation*

This section presents two selected flights that can be seen in Figure 8 and 9. Both Figures show the drone's flight path (in red), the estimated position of the POI (in blue) and the ground truth (in green). These flights were selected since they feature two simple movements (moving towards and orbiting around a POI) that are likely to occur during field observations. Moreover, both flights happen at an altitude of 120m above ground, which maximises the performance of the algorithm (see Section 4.4 and 4.9), thus showing how well

http://www.imavs.org/

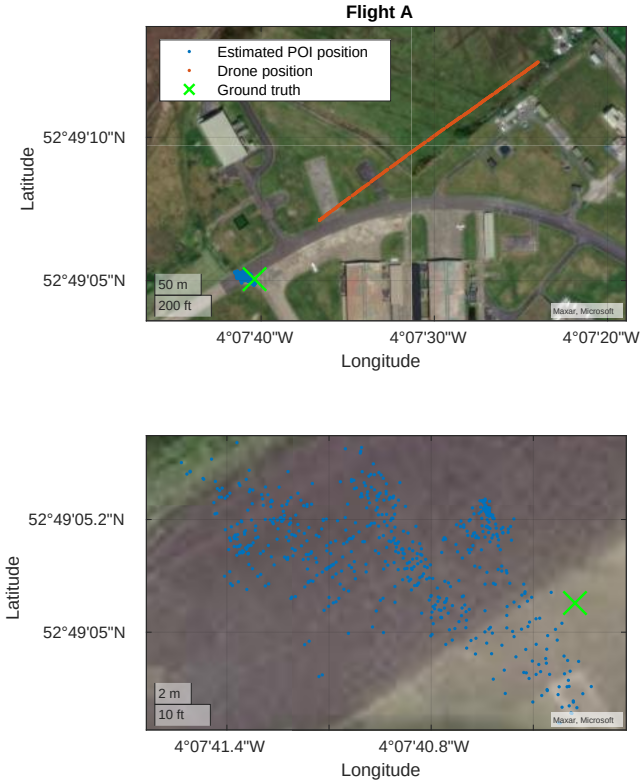

Figure 8: Straight flight towards the POI, altitude: 120m, distance to POI: 385m to 95m, max lateral error: 19.2m, max longitudinal error: 14.4m.

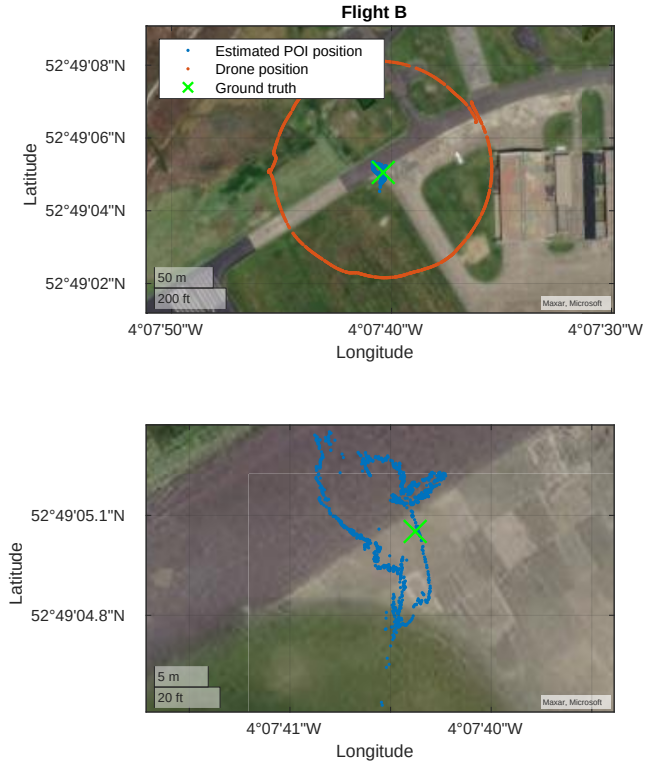

Figure 9: Orbit around the POI, altitude: 120m, distance to POI: 95m, max lateral error: 16.1m, max longitudinal error: 7.4m.

the algorithm can perform in good conditions. Both flights were processed taking into account the tuned focal length discussed in Section 4.5 and the time delay discussed in Section 4.6, but they are not corrected for the constant bias (see Section 7).

For flight A (Figure 8), it is interesting to note that at 385m the error is not larger than 19.2m laterally and 14.4m longitudinally. For flight B (Figure 9), flying at a distance of 95m to the POI, the error is reduced to 16.1m laterally and 7.4m longitudinally. However, there is a lot of structure in the estimated position, suggesting that there are camera movements not properly accounted for. It is likely that this results from the camera heading approximation discussed in Section 4.7.

5 CONCLUSION AND FUTURE WORK

In summary, this work presented a simple localisation algorithm that can be run on a commercial platform: the DJI Mavic 3E. The method has been successfully deployed in the Ol Pejeta Conservancy (Kenya) and at Llanbedr Airfield (Wales). The analysis of the data acquired led to a better understanding of the capabilities and limitations of this algorithm and platform. In particular:

- The estimation error can be reduced by ensuring that the camera is as close to vertical as the mission requirements allow it to be (Section 4.4).
- The estimation is sensitive to the knowledge of the camera focal length (Section 4.5). This can be mitigated by ensuring the POI is in the centre of the image.
- There are synchronisation issues between image and telemetry (Section 4.6).
- There is a constant heading and pitch bias, probably specific to each flight, that should be calibrated out (Section 4.8).

Based on these findings, this work also presented mission planning recommendations to improve the estimation accuracy (Section 4.9).

The resulting localisation error, for a POI 385m away, can be as good as 19.2m laterally and 14.4m longitudinally (Section 4.10).

Further work will address the shortcomings pointed out in the article, such as:

- Develop a more accurate camera model based on a better understanding of the DJI Mavic 3E's camera.
- Address the data synchronisation issue.

http://www.imavs.org/

http://www.imavs.org/

- Improve the pilot's user interface for better and safer control of the drone.
- Implement a gimbal calibration routine to determine heading and pitch biases.
- Account for terrain elevation during the localisation.
- Filter the estimation over time to improve localization precision.

ACKNOWLEDGEMENTS

This research has been carried out as part of the project WildDrone, funded by the European Union's Horizon Europe Research and Innovation Program under the Marie Skłodowska-Curie Grant Agreement No. 101071224. The WildDrone project has also received funding in part from the EPSRC funded Autonomous Drones for Nature Conservation Missions grant (EP/X029077/1). The authors would like to thank the Kenya Flying Labs, Kenya Civil Aviation Authority, the local Kenya Air Force ATC and the Wildlife Research and Training Institute for their support during the project.

REFERENCES

[1] N. Millner et al. "Exploring the opportunities and risks of aerial monitoring for biodiversity conservation". en. In: *Global Social Challenges Journal* 2.1 (June 2023). Publisher: Bristol University Press Section: Global Social Challenges Journal, pp. 2–23.

[2] M. Hoffmann et al. "The Impact of Conservation on the Status of the World's Vertebrates". In: *Science* 330.6010 (Dec. 2010). Publisher: American Association for the Advancement of Science, pp. 1503–1509.

[3] N. G. Yoccoz, J. D. Nichols, and T. Boulinier. "Monitoring of biological diversity in space and time". English. In: *Trends in Ecology & Evolution* 16.8 (Aug. 2001). Publisher: Elsevier, pp. 446–453. ISSN: 0169-5347.

[4] C. Vermeulen, P. Lejeune, J. Lisein, P. Sawadogo, and P. Bouché. "Unmanned Aerial Survey of Elephants". en. In: *PLOS ONE* 8.2 (Feb. 2013). Publisher: Public Library of Science, e54700. ISSN: 1932-6203.

[5] D. Wang, Q. Shao, and H. Yue. "Surveying Wild Animals from Satellites, Manned Aircraft and Unmanned Aerial Systems (UASs): A Review". en. In: *Remote Sensing* 11.11 (Jan. 2019). Number: 11 Publisher: Multidisciplinary Digital Publishing Institute, p. 1308. ISSN: 2072-4292.

[6] P. Bouché et al. "Game over! Wildlife collapse in northern Central African Republic". en. In: *Environmental Monitoring and Assessment* 184.11 (Nov. 2012), pp. 7001–7011. ISSN: 1573-2959.

[7] Z. Yang et al. "Spotting East African Mammals in Open Savannah from Space". en. In: *PLOS ONE* 9.12 (Dec. 2014). Publisher: Public Library of Science, e115989. ISSN: 1932-6203.

[8] I. Duporge, T. Hodgetts, T. Wang, and D. W. Macdonald. "The spatial distribution of illegal hunting of terrestrial mammals in Sub-Saharan Africa: a systematic map". en. In: *Environmental Evidence* 9.1 (June 2020), p. 15. ISSN: 2047-2382.

[9] R. Lamprey et al. "Comparing an automated high-definition oblique camera system to rear-seat-observers in a wildlife survey in Tsavo, Kenya: Taking multi-species aerial counts to the next level". In: *Biological Conservation* 241 (Jan. 2020), p. 108243. ISSN: 0006-3207.

[10] S. A. Wich and L. Pin Koh. "Mapping". In: *Conservation Drones: Mapping and Monitoring Biodiversity*. Ed. by S. A. Wich and L. P. Koh. Oxford University Press, June 2018, pp. 51–54. ISBN: 978-0-19-878761-7.

[11] L. P. Koh and S. A. Wich. "Dawn of Drone Ecology: Low-Cost Autonomous Aerial Vehicles for Conservation". en. In: *Tropical Conservation Science* 5.2 (June 2012). Publisher: SAGE Publications Inc, pp. 121–132. ISSN: 1940-0829.

[12] Wich. *Drones and Conservation. Drones and Aerial Observation: New Technologies for Property Rights*. en.

[13] E. Bondi et al. "BIRDSAI: A Dataset for Detection and Tracking in Aerial Thermal Infrared Videos". In: 2020, pp. 1747–1756.

[14] D. Chabot and D. M. Bird. "Evaluation of an off-the-shelf Unmanned Aircraft System for Surveying Flocks of Geese". In: *Waterbirds* 35.1 (Mar. 2012). Publisher: The Waterbird Society, pp. 170–174. ISSN: 1524-4695, 1938-5390.

[15] S. Wich, D. Dellatore, M. Houghton, R. Ardi, and L. P. Koh. "A preliminary assessment of using conservation drones for Sumatran orang-utan (*Pongo abelii*) distribution and density". en. In: *Journal of Unmanned Vehicle Systems* 4.1 (Mar. 2016), pp. 45–52. ISSN: 2291-3467.

[16] K. Whitehead et al. "Remote sensing of the environment with small unmanned aircraft systems (UASs), part 2: scientific and commercial applications". en. In: *Journal of Unmanned Vehicle Systems* 02.03 (Sept. 2014), pp. 86–102. ISSN: 2291-3467.

https://www.imavs.org/pdf/imav.2024.39

[17] J. S. Avila-Sanchez et al. "Evaluating the Use of a Thermal Sensor to Detect Small Ground-Nesting Birds in Semi-Arid Environments during Winter". en. In: *Drones* 8.2 (Feb. 2024). Number: 2 Publisher: Multidisciplinary Digital Publishing Institute, p. 64. ISSN: 2504-446X.

[18] M. D. Somers et al. *Airborne point counts: a method for estimating songbird abundance with drones*. en. Pages: 2020.08.15.252429 Section: New Results. Aug. 2020.

[19] W. Andrew et al. "Visual identification of individual Holstein-Friesian cattle via deep metric learning". en. In: *Computers and Electronics in Agriculture* 185 (June 2021), p. 106133. ISSN: 01681699.

[20] J. C. Hodgson et al. "Drones count wildlife more accurately and precisely than humans". en. In: *Methods in Ecology and Evolution* 9.5 (2018). _eprint: https://onlinelibrary.wiley.com/doi/pdf/10.1111/2041-210X.12974, pp. 1160–1167. ISSN: 2041-210X.

[21] C. Aubert et al. "Estimating Total Length of Partially Submerged Crocodylians from Drone Imagery". en. In: *Drones* 8.3 (Mar. 2024). Number: 3 Publisher: Multidisciplinary Digital Publishing Institute, p. 115. ISSN: 2504-446X.

[22] R. Viegut et al. "Detection Probability and Bias in Machine-Learning-Based Unoccupied Aerial System Non-Breeding Waterfowl Surveys". en. In: *Drones* 8.2 (Feb. 2024). Number: 2 Publisher: Multidisciplinary Digital Publishing Institute, p. 54. ISSN: 2504-446X.

[23] P. Povlsen, D. Bruhn, C. Pertoldi, and S. Pagh. "A Novel Scouring Method to Monitor Nocturnal Mammals Using Uncrewed Aerial Vehicles and Thermal Cameras—A Comparison to Line Transect Spotlight Counts". en. In: *Drones* 7.11 (Nov. 2023). Number: 11 Publisher: Multidisciplinary Digital Publishing Institute, p. 661. ISSN: 2504-446X.

[24] M. Jiménez-Torres, C. P. Silva, C. Riquelme, S. A. Estay, and M. Soto-Gamboa. "Automatic Recognition of Black-Necked Swan (Cygnus melancoryphus) from Drone Imagery". en. In: *Drones* 7.2 (Feb. 2023). Number: 2 Publisher: Multidisciplinary Digital Publishing Institute, p. 71. ISSN: 2504-446X.

[25] Q. Ye, J. Luo, and Y. Lin. "A coarse-to-fine visual geo-localization method for GNSS-denied UAV with oblique-view imagery". In: *ISPRS Journal of Photogrammetry and Remote Sensing* 212 (June 2024), pp. 306–322. ISSN: 0924-2716.

[26] Y. Chen and J. Jiang. "An Oblique-Robust Absolute Visual Localization Method for GPS-Denied UAV With Satellite Imagery". In: *IEEE Transactions on Geoscience and Remote Sensing* 62 (2024), pp. 1–13. ISSN: 0196-2892, 1558-0644.

[27] D. Saunders et al. "Radio-tracking wildlife with drones: a viewshed analysis quantifying survey coverage across diverse landscapes". en. In: *Wildlife Research* 49.1 (Feb. 2022). Publisher: CSIRO PUBLISHING, pp. 1–10. ISSN: 1448-5494.

[28] R. Rodriguez, D. M. Jenkins, J. Leary, and R. Perroy. "A direct geolocation method for aerial imaging surveys of invasive plants". en. In: *International Journal of Environmental Science and Technology* (Apr. 2024). ISSN: 1735-2630.

[29] JARUS. *JARUS guidelines on Specific Operations Risk Assessment (SORA)*. May 2024.

http://www.imavs.org/